Original article

Kriging-based subdivision schemes: Application to the reconstruction of non-regular environmental data

Jean Baccou [a], Jacques Liandrat [b],*

[a] *IRSN, Centre de Cadarache, 13115 Saint Paul-Lez-Durance, France*
[b] *Centrale Marseille and LATP, Technopôle de Château-Gombert, 13451 Marseille Cedex 20, France*

Abstract

This work is devoted to the construction of new kriging-based interpolating position-dependent subdivision schemes for data reconstruction. Their originality stands in the coupling of the underlying multi-scale framework associated to subdivision schemes with kriging theory. Thanks to an efficient stencil selection, they allow to cope the problem of non-regular data prediction while keeping the interesting properties of kriging operators for the quantification of prediction errors. The proposed subdivision schemes are fully analyzed and an application to the reconstruction of non-regular environmental data is given as well.
© 2011 IMACS. Published by Elsevier B.V. All rights reserved.

Keywords: Kriging; Subdivision scheme; Non-regular data prediction

1. Introduction

Data modeling methods play a key role in the treatment of environmental problems. The information about the phenomenon under study is often discrete since it is provided by experimental measurements or numerical processing and therefore, modeling (or prediction) is required. Among data modeling methods, stochastic kriging-based approaches [7] are often used. Their main advantages compared to deterministic methods stand in the possibility to quantify the precision of the prediction thanks to an underlying probabilistic model. However, these methods usually assume that the phenomenon to predict is regular, which is not the case in practice such as in risk analysis where reliable reconstruction methods are crucial for the decision-making process. This paper is therefore devoted to the design of new stochastic modeling methods that improve the accuracy of the reconstruction of non-regular data. Contrary to classical approaches, their construction will be performed in two steps: a segmentation of data into different zones and a local kriging-based data prediction according to the information coming from the previous step. Taking apart the problem of data segmentation that refers to the wide literature of edge detector, we focus in the sequel on the construction of a new kriging-based subdivision scheme [8] for data prediction integrating local strategy according to the segmentation. Our work is organized as follows: Section 2 deals with the construction of our new subdivision schemes. Convergence results are provided in Section 3. Section 4 is devoted to applications to synthetic or real data.

* Corresponding author.
  E-mail addresses: jean.baccou@irsn.fr (J. Baccou), jliandrat@ec-marseille.fr, jacques.liandrat@ec-marseille.fr (J. Liandrat).

2. Kriging-based position dependent prediction

In this section, we plug the kriging interpolation into the Harten's subdivision framework [10].

2.1. Harten's framework

The general Harten's setting is a family of triplets $(V^j, D_j^{j-1}, P_{j-1}^j)$ where $j \in \mathbb{Z}$ is a scale parameter. For each value of j, V^j denotes a separable space of approximation associated to a resolution level 2^{-j}, D_j^{j-1} (resp. P_{j-1}^j) is a decimation (resp. prediction) operator connecting V^j to V^{j-1} (resp. V^{j-1} to V^j). Usually, these two operators are constructed from the pairs (D_j, R_j) of discretization and reconstruction operators as $P_{j-1}^j = D_j R_{j-1}$ and $D_j^{j-1} = D_{j-1} R_j$.

Since the prediction operator P_{j-1}^j maps any element of V^{j-1} in an element of V^j, it defines a subdivision scheme [8] that reads $\forall \{f_k^{j-1}\}_{k \in \mathbb{Z}}$, $(P_{j-1}^j f^{j-1})_k = \sum_{m \in \mathbb{Z}} a_{k-2m}^{j,k} f_m^{j-1}$. Here, $\{a_{k-2m}^{j,k}\}_{m \in \mathbb{Z}}$, $(j, k) \in \mathbb{Z}^2$ is called the mask of the subdivision scheme. If it is independent of f^{j-1}, the subdivision is said to be linear. Moreover, one speaks about stationarity (resp. uniformity) when the mask does not depend on j (resp. on k).

The design of prediction operators is crucial for data reconstruction. As mentioned before, it depends on the discretization and reconstruction operators. From now on, we assume that D_j is the sampling operator defined by $(D_j f)_k = f(x_k^j)$ with $x_k^j = k2^{-j}$.

Here, we define a reconstruction operator based on kriging interpolation.

2.2. A quick overview of kriging interpolation

Kriging interpolation [7,13,9] belongs to the class of stochastic methods. Starting from an initial set of data, denoted $\{f(x_i)\}_{i=1,...,N}$, it is assumed that each $f(x_i)$ is a realization of a random variable $\mathcal{F}(x_i)$, the subset $\{\mathcal{F}(x_i), i = 1, \ldots, N\}$ coming from a random process $\mathcal{F}(x)$ satisfying $\mathcal{F}(x) = m(x) + \delta(x)$. $m(x)$ is the deterministic mean structure of $\mathcal{F}(x)$ and $\delta(x)$ is a zero-mean random process which can be spatially correlated. Denoting $x^\star$ a new location, the prediction of $f(x^\star)$, from $\{f(x_i)\}_{i=1,...,N}$ is therefore performed in two steps: the first one consists in identifying the spatial correlation associated to $\delta(x)$ while the second one is an interpolation step based on this spatial correlation.

Step 1: Under stationarity assumptions and constant deterministic mean structure of the random process, the spatial correlation structure associated to $\delta(x)$ is the spatial correlation of the random process $\mathcal{F}(x)$. It is exhibited by computing the semi-variogram, $\gamma(h) = 1/2 E((\mathcal{F}(x + h) - \mathcal{F}(x))^2)$, where E denotes the mathematical expectation.

Exploiting the information provided by the observed data $\{f(x_i)\}_{i=1,...,N}$, it is approximated by a fit of the discrete experimental semi-variogram, $\gamma_{\exp}(h) = 1/(2 \operatorname{Card}(N(h))) \sum_{(k,l) \in N(h)} (f(x_k) - f(x_l))^2$, with $N(h) = \{(x_k, x_l), h - \epsilon \leq |x_k - x_l| \leq h + \epsilon\}$) and for every h such that $\operatorname{Card}(N(h))$, the cardinality of $N(h)$, is sufficiently large.

Step 2: The interpolation step is based on the minimization of the estimation variance $var (\mathcal{F}(x^\star) - P(\mathcal{F}, x^\star))$ where $P(\mathcal{F}, x^\star)$ is an estimator of $\mathcal{F}(x^\star)$ satisfying the unbiasedness constraint $E(P(\mathcal{F}, x^\star)) = E(\mathcal{F}(x^\star))$. Kriging approach focusses on linear estimators i.e. $P(\mathcal{F}, x^\star) = \sum_{i=1}^N \lambda_i(x^\star)\mathcal{F}(x_i)$ with $\{\lambda_i(x^\star)\}_{i=1,...,N}$ the kriging weights. Therefore, it yields to optimal linear predictor.

Under linearity of the estimator, the estimation variance depends only on the kriging weights and on the semi-variogram identified in the first step. The minimization problem can then be reformulated under the following matricial equation:

$$\begin{bmatrix} \gamma(0) & \ldots & \gamma(|x_1 - x_N|) & 1 \\ \gamma(|x_2 - x_1|) & \ldots & \gamma(|x_2 - x_N|) & 1 \\ \ldots & \ldots & \ldots & \ldots \\ \gamma(|x_N - x_1|) & \ldots & \gamma(0) & 1 \\ 1 & \ldots & 1 & 0 \end{bmatrix} \begin{bmatrix} \lambda_1(x^\star) \\ \lambda_2(x^\star) \\ \ldots \\ \lambda_N(x^\star) \\ \mu \end{bmatrix} = \begin{bmatrix} \gamma(|x_1 - x^\star|) \\ \gamma(|x_2 - x^\star|) \\ \ldots \\ \gamma(|x_N - x^\star|) \\ 1 \end{bmatrix}, \tag{1}$$

with μ the Lagrange multiplier enforcing the unbiasedness of the estimator.

Many interpolation techniques are used in environmental studies. Among the most popular ones, we can mention the Inverse Distance Weighted interpolation (IDW) which computes the approximation of $f(x^\star)$ as a linear combination

of the observed data taking into account the distance between $x^\star$ and $\{x_i\}_{i=1,\ldots,N}$. Despite the similarities in the construction between this approach and kriging interpolation, there exists three main differences that motivate our work in the kriging framework.

- Integration of the spatial correlation in the interpolation: contrary to IDW, kriging interpolation exploits the information provided by the observed data (semi-variogram). This is an important point for the construction of an interpolation model that faithfully approximates the phenomenon to predict. It avoids artificial choices which could reduce the confidence in the obtained values.
- Robustness of the interpolation with regards to discretization: similarly to IDW, the computation of the kriging weights takes into account the relative position of the points to interpolate compared to the observed data (right hand side of System (1)) but it also depends on the relative position between data themselves (left hand side of System (1)). As a result, the kriging estimator is more robust to a non-uniform discretization, reducing the overestimation of the influence of clusters usually encountered with IDW.
- Error estimation: thanks to the computation of the estimation variance, kriging interpolation provides a local prediction error. This last point is crucial in the environmental studies conducted by the French Institut de Radioprotection et de Sûreté Nucléaire which is in charge of safety assessment. Since the estimation error depends on the identification of the semi-variogram, it brings significant information to the analyst about modelling effects. It is also an important tool to ensure transparency in the results that are used to inform the population about potential danger.

Therefore, kriging interpolation appears to be an efficient approach for data prediction, particularly well suited for our applications (see Section 4.2). Moreover, thanks to the flexibility of its construction, it can be adapted to the case of non-regular data, which is our concern in this paper, by taking into account in the kriging problem (1) a subset of data $\{f(x_i)\}_{i \in I^\star}$ close to the new location instead of the whole ones. The integration of locality in the prediction and its plugging in the Harten's framework are fully described in the next section.

2.3. Coupling Kriging interpolation and Harten's multiresolution

Coming back to the Harten's framework, we propose to use kriging interpolation to connect two successive approximation spaces V^j, V^{j+1}. Keeping in mind that the rest of the paper is devoted to non-regular data prediction, this interpolation is performed locally. More precisely, for every scale j, one associates to any new location $x^\star \in [x_{k-1}^j x_k^j]$ an interpolating stencil $\{x_{k-l(x^\star)}^j, \ldots, x_{k+r(x^\star)-1}^j\}$. The parameter $l(x^\star)$ (resp. $r(x^\star)$) denotes the number of left (resp. right) points in the interpolating stencil such that $l(x^\star) + r(x^\star) = D + 1$ ($D \in \mathbb{N}$).

Assuming that the semi-variogram has been identified once and for all from the available data, the kriging-based reconstruction operator is finally defined, for any integer D, as a piecewise interpolation operator such that for all $f^j \in V^j$,

$$R_j f^j(x) = \sum_{m=-l(x)}^{r(x)-1} \lambda_{j,m}^{l(x),r(x)-1}(x) f_{k+m}^j, \quad \text{if } x \in [(k-1)2^{-j}, k2^{-j}]. \tag{2}$$

The kriging weights, $\{\lambda_{j,m}^{l(x),r(x)-1}(x)\}_m$ are solutions of Problem (1) where $\{x_1, \ldots, x_N\}$ is replaced by $\{x_{k-l(x)}^j, \ldots, x_{k+r(x)-1}^j\}$.

The kriging-based prediction operator associated to the reconstruction (2) is then defined for all $k \in \mathbb{Z}$ as:

$$\begin{cases} f_{2k}^{'j+1} = (P_j^{j+1} f^{'j})_{2k} = f_k^{'j}, \\ f_{2k-1}^{'j+1} = (P_j^{j+1} f^{'j})_{2k-1} = \sum_{m=-l_{j+1,2k-1}}^{r_{j+1,2k-1}-1} \lambda_{j,m}^{l_{j+1,2k-1},r_{j+1,2k-1}-1} f_{k+m}^{'j}, \end{cases} \tag{3}$$

where $\forall k \in \mathbb{Z}$, $f_k^{'0} = f_k^0$ and $\{\lambda_{j,m}^{l_{j+1,2k-1},r_{j+1,2k-1}-1}\}_m$ are the kriging weights when $x = x_{2k-1}^{j+1}$ (therefore $l_{j+1,2k-1} = l(x_{2k-1}^{j+1})$ and $r_{j+1,2k-1} = r(x_{2k-1}^{j+1})$).
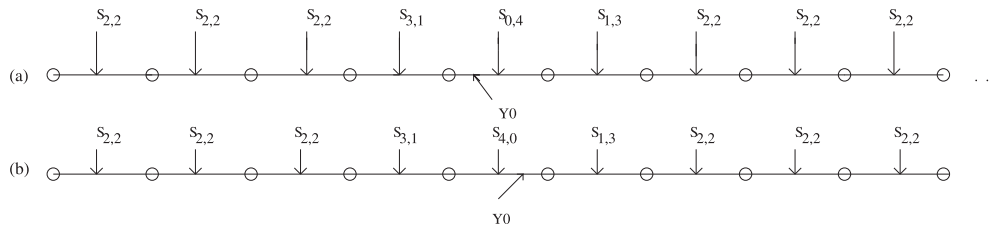
Fig. 1. Example of stencil selection associated to a unique segmentation point $y_0 \in [x_{k_{j-1}-1}^{j-1}, x_{k_{j-1}}^{j-1}]$, $S_{l,r}$ stands for the stencil with l left points and r right points. (a) $y_0 \in [x_{2k_{j-1}-2}^{j}, x_{2k_{j-1}-1}^{j}]$ and (b) $y_0 \in [x_{2k_{j-1}-1}^{j}, x_{2k_{j-1}}^{j}]$.

System (3) appears as a subdivision scheme with the mask:

$$
a^{j,2k} : \begin{cases} a_0^{j,2k} = 1, \\ a_m^{j,2k} = 0, \ m \neq 0, \end{cases}
\quad , \quad
a^{j,2k-1} : \begin{cases} a_{-2m-1}^{j,2k-1} = \lambda_{j-1,m}^{l_{j,2k-1},r_{j,2k-1}}, \\ \text{for } m = -l_{j,2k-1}, \dots, r_{j,2k-1} - 1, \\ a_m^{j,2k-1} = 0 \text{ otherwise.} \end{cases}
$$

Given (D, l, r) with $l + r = D + 1$, there are many strategies to define the couple $(l_{j,2k-1}, r_{j,2k-1})$. Among them, one mentions the two following ones that will be considered in this paper. The first one is $l_{j,2k-1} = l$, $r_{j,2k-1} = r$ that leads to translation-invariant stencils. The corresponding subdivision scheme is then stationary and uniform. In the second strategy, $(l_{j,2k-1}, r_{j,2k-1})$ are functions of an a priori defined segmentation of the real line. This leads to position-dependent stencils and defines non-stationary and non-uniform subdivision scheme. In this case and since our goal is the approximation of piecewise smooth functions, we focus for the rest of the paper on the following position-dependent stencil selection, associated to a unique segmentation point $\{y_0\}$.

Definition 2.1. Let us define for all $j \in \mathbb{Z}$, the index k_{j-1} s.t. $y_0 \in [x_{k_{j-1}-1}^{j-1}, x_{k_{j-1}}^{j-1}]$. For all j and k such that $y_0 \in [x_{-l+k}^{j-1}, x_{r-1+k}^{j-1}]$, we set:

- If $y_0 \in [x_{2k_{j-1}-2}^{j}, x_{2k_{j-1}-1}^{j}]$, then

$$
\begin{cases}
\text{If } k < k_{j-1} \text{ then} \\
r_{j,2k-1} = k_{j-1} - k \text{ and } l_{j,2k-1} = D + 1 - k_{j-1} + k, \\
\text{If } k \geq k_{j-1} \text{ then} \\
r_{j,2k-1} = D + 1 + k_{j-1} - k \text{ and } l_{j,2k-1} = k - k_{j-1}.
\end{cases}
$$

- If $y_0 \in [x_{2k_{j-1}-1}^{j}, x_{2k_{j-1}}^{j}]$, then

$$
\begin{cases}
\text{If } k \leq k_{j-1} \text{ then} \\
r_{j,2k-1} = k_{j-1} - k \text{ and } l_{j,2k-1} = D + 1 - k_{j-1} + k, \\
\text{If } k > k_{j-1} \text{ then} \\
r_{j,2k-1} = D + 1 + k_{j-1} - k \text{ and } l_{j,2k-1} = k - k_{j-1}.
\end{cases}
$$

Fig. 1 displays an example of this selection rule when $D = 3$, $l = 2$ and $r = 2$.

The proposed kriging-based position-dependent prediction turns out to be an efficient approach for the prediction of non-regular data for the following reasons: by construction, it benefits from the same advantages as kriging i.e. integration of spatial data structure, error estimation (depending on the local semi-variogram and on

the distance between the points involved in the kriging system) and robustness to discretization. This last advantage is important when we intend to interpolate on a locally refined dyadic grid as it is proposed in [5]. Moreover, the data segmentation allows to specify the prediction in each zone of the domain and to take into account the position of the point inside its zone. Therefore, if the segmentation points fit exactly with the position of discontinuities, as proved in [4], the limit function (that exists according to the following section) does not exhibit oscillations characteristic of the Gibbs phenomenon associated to interpolatory linear translation invariant high order subdivision.

Remark 2.1. Position dependency is not the only way to avoid Gibbs oscillations and various nonlinear strategies have been developed (see for instance [2] or [1]). The coupling of kriging with ENO strategy could be performed; however, there is no clear strategy to embed in a same scheme kriging and PPH approaches.

3. Convergence analysis of the kriging-based subdivision scheme

We first recall the classical definition of uniform convergence for stationary subdivision schemes [8].

Definition 3.1. The subdivision scheme $\mathcal{S}$ is said to be L^∞-convergent if for any real sequence $\{f_k^0\}_{k \in \mathbb{Z}} \in V^0$, there exists a continuous function f (called the limit function associated to f^0) such that: $\forall \epsilon$, $\exists J$ such that $\forall j \geq J$, $\|\mathcal{S}^j f^0 - f(\cdot/2^j)\|_\infty \leq \epsilon$.

In the case of position-dependent subdivision scheme, the previous definition is slightly modified since the adaptation of the prediction around segmentation points can lead to discontinuous limit functions. We refer to [4] for further details.

Among the various tools available to establish the convergence of a subdivision scheme the so called matrix formalism [11] has been generalized in [4] to non-uniform schemes. In order to study the convergence of kriging-based subdivision schemes, we propose in what follows an extension to non-stationary prediction.

3.1. General convergence results

Extending [8,4], it turns out to be that one can associate to a non-stationary and non-uniform scheme, a set of refinement matrices for a translation-invariant strategy and a set of refinement and edge matrices (due to subdivision around segmentation points) when choosing the previously defined position-dependent scheme. More precisely, we have:

Definition 3.2.

- For a translation-invariant subdivision, let F_k^j be the minimal set of N points at level j that determines the values at dyadic points in the interval $[k2^{-j}, (k+1)2^{-j}]$ at level above j. For each j, the two $N \times N$ refinement matrices, $A_{0,j}$ and $A_{1,j}$ are defined by $F_{2k}^{j+1} = A_{0,j}F_k^j$ and $F_{2k+1}^{j+1} = A_{1,j}F_k^j$.
- Around segmentation points, let G_+^j (resp. G_-^j) be the set of M points at level j that determines the corresponding set of points G_+^{j+1} (resp. G_-^{j+1}) in the right (resp. left) vicinity of y_0. For each j, the two $M \times M$-edge matrices $A_{2,j}^+$ and $A_{2,j}^-$ are defined by $G_-^{j+1} = A_{2,j}^- G_-^j$ and $G_+^{j+1} = A_{2,j}^+ G_+^j$.

According to [4], the subdivision scheme is then completely characterized in the translation-invariant strategy by the set of refinement matrices $\{A_{0,j}, A_{1,j}\}_{j \in \mathbb{Z}}$. In the position-dependent strategy, it is characterized by the two sets of refinement/edge matrices $\{A_{0,j}, A_{1,j}\}_{j \in \mathbb{Z}}/\{A_{2,j}^-, A_{2,j}^+\}_{j \in \mathbb{Z}}$ and, for any dyadic point $x = k_x 2^{-j_x}$ ($x \neq y_0$), by the integer T_x corresponding to the length of the range of scales where the two successive differences, $\delta f_{k2^{j-j_x}}^j$ and $\delta f_{k2^{j-j_x}-1}^j$, are computed mixing refinement and edge matrices (we note $\delta f_k = f_{k+1} - f_k$).

Following [8,4] we also introduce, for each j, $A_{0,j}^{(1)}$ and $A_{1,j}^{(1)}$ (resp. $A_{2,j}^{(1),-}$ and $A_{2,j}^{(1),+}$) the refinement (resp. edge) matrices of the subdivision scheme associated to the first difference.

The following convergence theorem then holds:

Theorem 3.1. *Translation-invariant strategy*:
If there exists J and μ_0 such that,

$$\left\| \Pi_{m \le J} \frac{1}{2} A_{\epsilon,m}^{(1)} \right\|_\infty \le \mu_0 < 1, \quad \text{for all } \epsilon \in \{0, 1\}, \tag{4}$$

then the translation-invariant subdivision scheme is uniformly convergent.
Position-dependent strategy:
If there exists J, μ_0 and T such that,

$$\left\| \Pi_{m \le J} \frac{1}{2} A_{\epsilon,m}^{(1)} \right\|_\infty \le \mu_0 < 1, \quad \text{for all } \epsilon \in \{0, 1\}, \tag{5}$$

$$\left\| \Pi_{m \le J} \frac{1}{2} A_{2,m}^{(1),-} \right\|_\infty \le \mu_0 < 1, \quad \left\| \Pi_{m \le J} \frac{1}{2} A_{2,m}^{(1),+} \right\|_\infty \le \mu_0 < 1, \tag{6}$$

and $\forall x$, $T_x \le T < \infty$, then the position-dependent subdivision scheme is uniformly convergent.

3.2. Two examples of convergence analysis

This section is devoted to the study of the convergence of two kriging-based subdivision schemes with parameters (3, 2, 2). They correspond to two different identified semi-variograms that are used in the numerical tests of Section 4.

3.2.1. Exponential semi-variogram

We assume here that the semi-variogram identified from the data is of exponential type i.e. $\gamma(h) = K\left(1 - e^{-ah}\right)$ (K and $a > 0$). In order to prove the uniform convergence, we start by studying in the two next propositions the asymptotical subdivision scheme obtained to the limit of large values of j. Then, we derive the convergence result for the subdivision scheme itself.

Proposition 3.1. *The kriging weights involved in the translation-invariant and position-dependent subdivision schemes with an exponential semi-variogram satisfy:*

$$(\lambda_{j,-2}^{2,2}, \lambda_{j,-1}^{2,2}, \lambda_{j,0}^{2,2}, \lambda_{j,1}^{2,2}) \xrightarrow{j \to +\infty} \left(0, \frac{1}{2}, \frac{1}{2}, 0\right), \tag{7}$$

$$(\lambda_{j,2}^{1,3}, \lambda_{j,1}^{1,3}, \lambda_{j,0}^{1,3}, \lambda_{j,-1}^{1,3}) = (\lambda_{j,-3}^{3,1}, \lambda_{j,-2}^{3,1}, \lambda_{j,-1}^{3,1}, \lambda_{j,0}^{3,1}) \xrightarrow{j \to +\infty} \left(0, 0, \frac{1}{2}, \frac{1}{2}\right), \tag{8}$$

$$(\lambda_{j,3}^{0,4}, \lambda_{j,2}^{0,4}, \lambda_{j,1}^{0,4}, \lambda_{j,0}^{0,4}) = (\lambda_{j,-4}^{4,0}, \lambda_{j,-3}^{4,0}, \lambda_{j,-2}^{4,0}, \lambda_{j,-1}^{4,0}) \xrightarrow{j \to +\infty} (0, 0, 0, 1). \tag{9}$$

Proof. Here $D = 3$ and $(r, l) \in \{(2, 2), (3, 1), (4, 0), (1, 3), (0, 4)\}$. We focus on (7), the proofs for (8) and (9) being similar.

Since we are interested in the behavior of the kriging weights when $j \to \infty$, one writes $\gamma(h) = Kah + O(h^2)$. Then, the kriging system (1) becomes:

$$(\Gamma_{j,4}^0 + \Gamma_{j,4}^1)\Lambda_j = \gamma_{j,4}^0 + \gamma_{j,4}^1, \tag{10}$$

where the matrix $\Gamma_{j,4}^0$ (resp. $\Gamma_{j,4}^1$) stands for the first order (resp. second order) term with regards to h powers.

More precisely,

$$
\Gamma_{j,4}^0 = \begin{bmatrix} 0 & a2^{-j} & 2a2^{-j} & 3a2^{-j} & 1 \\ a2^{-j} & 0 & a2^{-j} & 2a2^{-j} & 1 \\ 2a2^{-j} & a2^{-j} & 0 & a2^{-j} & 1 \\ 3a2^{-j} & 2a2^{-j} & a2^{-j} & 0 & 1 \\ 1 & 1 & 1 & 1 & 0 \end{bmatrix}, \quad \gamma_{j,4}^0 = \begin{bmatrix} \frac{3}{2}a2^{-j} \\ \frac{1}{2}a2^{-j} \\ \frac{1}{2}a2^{-j} \\ \frac{3}{2}a2^{-j} \\ 1 \end{bmatrix}.
$$

It is elementary to show that:

$$
\|\Gamma_{j,4}^1\|_\infty < K_{\Gamma^1} 2^{-2j} \quad \text{and} \quad \|\gamma_{j,4}^1\|_\infty < K_{\gamma^1} 2^{-2j}. \tag{11}
$$

The solution of (10) is then:

$$
\Lambda_j = (I_4 + \Gamma_{j,4}^{0,-1}\Gamma_{j,4}^1)^{-1}\Gamma_{j,4}^{0,-1}\gamma_{j,4}^0 + (I_4 + \Gamma_{j,4}^{0,-1}\Gamma_{j,4}^1)^{-1}\Gamma_{j,4}^{0,-1}\gamma_{j,4}^1, \tag{12}
$$

where I_4 is the 4×4 identity matrix. We start by expanding $(I_4 + \Gamma_{j,4}^{0,-1}\Gamma_{j,4}^1)^{-1}$.

- Expansion of $(I_4 + \Gamma_{j,4}^{0,-1}\Gamma_{j,4}^1)^{-1}$

  From a classical result of matrix calculus,

$$
\Gamma_{j,4}^{0,-1} = \begin{bmatrix} B^{-1}(I_3 + 11'S^{-1}11B^{-1}) & -B^{-1}11'S^{-1} \\ -S^{-1}11B^{-1} & S^{-1} \end{bmatrix}.
$$

with

$$
B = 2^{-j}\begin{bmatrix} 0 & a & 2a & 3a \\ a & 0 & a & 2a \\ 2a & a & 0 & a \\ 3a & 2a & a & 0 \end{bmatrix}, \quad 11 = (1, 1, 1, 1) \text{ and } S = -11B^{-1}11'.
$$

From these definitions, it is then straightforward that $B^{-1}(I_3 + 11'S^{-1}11B^{-1}) = 2^j\mathcal{M}_1$, $B^{-1}11'S^{-1} = \mathcal{V}_2$, $(S^{-1}11B^{-1})' = \mathcal{V}_3$, and $S^{-1} = K_4 2^{-j}$ where $\mathcal{M}_1$, $\mathcal{V}_2$, $\mathcal{V}_3$ and K_4 are independent of j.

Therefore, $\|\Gamma_{j,4}^{0,-1}\|_\infty \leq K_{\Gamma^0}2^j$. Combined with (11) it gives

$$
\|\Gamma_{j,4}^{0,-1}\Gamma_{j,4}^1\|_\infty \leq K_{\Gamma^0}K_{\Gamma^1}2^{-j}, \tag{13}
$$

and finally, for sufficiently large j $(I_4 + \Gamma_{j,4}^{0,-1}\Gamma_{j,4}^1)^{-1} = \sum_{i=0}^\infty (-1)^i(\Gamma_{j,4}^{0,-1}\Gamma_{j,4}^1)^i$.

Expression (12) becomes:

$$
\Lambda_j = \Gamma_{j,4}^{0,-1}\gamma_{j,4}^0 + \sum_{i=1}^\infty (-1)^i(\Gamma_{j,4}^{0,-1}\Gamma_{j,4}^1)^i\Gamma_{j,4}^{0,-1}\gamma_{j,4}^0 + \sum_{i=0}^\infty (-1)^i(\Gamma_{j,4}^{0,-1}\Gamma_{j,4}^1)^i\Gamma_{j,4}^{0,-1}\gamma_{j,4}^1. \tag{14}
$$

Note that this step also provides the following inequalities that are useful in the sequel:

$$
\|\Gamma_{j,4}^{0,-1}\gamma_{j,4}^0\|_\infty \leq \mathcal{K}_0, \quad \|\Gamma_{j,4}^{0,-1}\gamma_{j,4}^1\|_\infty \leq \mathcal{K}_1 2^{-j}. \tag{15}
$$

Coming back to (14), in order to conclude the proof, we now show that the norm of second term tends to 0 when $j \to +\infty$, that the first term does not depend on j and that its four first components are equal to (0, 1/2, 1/2, 0).

Let us first focus on the second terms of (14). From (13) and (15), it is straightforward that:

$$\left\| \sum_{i=1}^{\infty} (-1)^i (\Gamma_{j,4}^{0,-1} \Gamma_{j,4}^1)^i \Gamma_{j,4}^{0,-1} \gamma_{j,4}^0 \right\|_{\infty} \leq \mathcal{K}_0 \sum_{i=1}^{\infty} (K_{\Gamma^0} K_{\Gamma^1})^i 2^{-ij},$$

$$\left\| \sum_{i=0}^{\infty} (-1)^i (\Gamma_{j,4}^{0,-1} \Gamma_{j,4}^1)^i \Gamma_{j,4}^{0,-1} \gamma_{j,4}^1 \right\|_{\infty} \leq \mathcal{K}_1 2^{-j} \sum_{i=0}^{\infty} (K_{\Gamma^0} K_{\Gamma^1})^i 2^{-ij},$$

which becomes for sufficiently large j,

$$\left\| \sum_{i=1}^{\infty} (-1)^i (\Gamma_{j,4}^{0,-1} \Gamma_{j,4}^1)^i \Gamma_{j,4}^{0,-1} \gamma_{j,4}^0 \right\|_{\infty} \leq \mathcal{K}_0 K_{\Gamma^0} K_{\Gamma^1} \frac{2^{-j}}{1 - K_{\Gamma^0} K_{\Gamma^1} 2^{-j}},$$

$$\left\| \sum_{i=0}^{\infty} (-1)^i (\Gamma_{j,4}^{0,-1} \Gamma_{j,4}^1)^i \Gamma_{j,4}^{0,-1} \gamma_{j,4}^1 \right\|_{\infty} \leq \mathcal{K}_1 \frac{2^{-j}}{1 - K_{\Gamma^0} K_{\Gamma^1} 2^{-j}}.$$

Therefore

$$\lim_{j \to \infty} \left\| \sum_{i=1}^{\infty} (-1)^i (\Gamma_{j,4}^{0,-1} \Gamma_{j,4}^1)^i \Gamma_{j,4}^{0,-1} \gamma_{j,4}^0 + \sum_{i=0}^{\infty} (-1)^i (\Gamma_{j,4}^{0,-1} \Gamma_{j,4}^1)^i \Gamma_{j,4}^{0,-1} \gamma_{j,4}^1 \right\|_{\infty} = 0.$$

For the first terms of (14), since by construction $\Gamma_{j,4}^0$ is invertible, the vector U is solution of $\Gamma_{j,4}^0 U = \gamma_{j,4}^0$. Direct calculation gives $U = (0, 1/2, 1/2, 0, 0)$, that concludes the proof. □

Using (7)–(9) one gets the following result:

Proposition 3.2. *The matrices involved in the asymptotical subdivision process are:*

(1) *Refinement matrices:*

$$A_0 = \begin{bmatrix} 0 & 1 & 0 & 0 & 0 & 0 \\ 0 & \frac{1}{2} & \frac{1}{2} & 0 & 0 & 0 \\ 0 & 0 & 1 & 0 & 0 & 0 \\ 0 & 0 & \frac{1}{2} & \frac{1}{2} & 0 & 0 \\ 0 & 0 & 0 & 1 & 0 & 0 \\ 0 & 0 & 0 & \frac{1}{2} & \frac{1}{2} & 0 \end{bmatrix}, \quad A_1 = \begin{bmatrix} 0 & \frac{1}{2} & \frac{1}{2} & 0 & 0 & 0 \\ 0 & 0 & 1 & 0 & 0 & 0 \\ 0 & 0 & \frac{1}{2} & \frac{1}{2} & 0 & 0 \\ 0 & 0 & 0 & 1 & 0 & 0 \\ 0 & 0 & 0 & \frac{1}{2} & \frac{1}{2} & 0 \\ 0 & 0 & 0 & 0 & 1 & 0 \end{bmatrix}$$

with $Sp(A_0) = Sp(A_1) = \{1, \frac{1}{2}, 0\}$.

(2) *Edge matrices: their expression depend on the dyadic decomposition of y_0,*

$$A_2^- \in \left\{ \begin{bmatrix} 0 & \frac{1}{2} & \frac{1}{2} & 0 \\ 0 & 0 & 1 & 0 \\ 0 & 0 & \frac{1}{2} & \frac{1}{2} \\ 0 & 0 & 0 & 1 \end{bmatrix}, \begin{bmatrix} 0 & 0 & 1 & 0 \\ 0 & 0 & \frac{1}{2} & \frac{1}{2} \\ 0 & 0 & 0 & 1 \\ 0 & 0 & 0 & 1 \end{bmatrix} \right\},$$

and

$$A_2^+ \in \left\{ \begin{bmatrix} 1 & 0 & 0 & 0 \\ 1 & 0 & 0 & 0 \\ \dfrac{1}{2} & \dfrac{1}{2} & 0 & 0 \\ 0 & 1 & 0 & 0 \end{bmatrix}, \begin{bmatrix} 1 & 0 & 0 & 0 \\ \dfrac{1}{2} & \dfrac{1}{2} & 0 & 0 \\ 0 & 1 & 0 & 0 \\ 0 & \dfrac{1}{2} & \dfrac{1}{2} & 0 \end{bmatrix} \right\}.$$

In any case, $Sp(A_2^+) \subset \{1, 1/2, 0\}$ and $Sp(A_2^-) \subset \{1, 1/2, 0\}$.

Proposition 3.2 finally leads to the convergence result.

Proposition 3.3. *The translation-invariant and position-dependent subdivision schemes of parameter* $(3, 2, 2)$ *associated to an exponential semi-variogram are uniformly convergent.*

Proof. Following [8], the eigenvalues of $(1/2)A_0^{(1)}$ and $(1/2)A_1^{(1)}$ (resp. $(1/2)A_2^{(1),-}$ and $(1/2)A_2^{(1),+}$) are the eigenvalues of A_0 and A_1 (resp. A_2^- and A_2^+) except $\lambda_0 = 1$. Thus, from Proposition 3.2, these eigenvalues are strictly bounded by 1. This is enough to ensure Inequalities (4), (5) and (6) for the asymptotical subdivision scheme and therefore for the subdivision scheme. Theorem 3.1 finally leads to the uniform convergence of the translation-invariant scheme but also to the position-dependent one since the extra assumption related to the uniform bound for the transition zone is satisfied following Proposition 2.3 of [4]. □

3.2.2. Gaussian semi-variogram

We assume here that the semi-variogram identified from the data is $\gamma(h) = K(1 - e^{-(ah)^2})$ (K and $a > 0$). As previously, the uniform convergence is established by first studying the asymptotical behavior of the scheme.

Proposition 3.4. *The kriging weights involved in the translation-invariant and position-dependent subdivision schemes with a Gaussian semi-variogram satisfy:*

$$(\lambda_{j,-2}^{2,2}, \lambda_{j,-1}^{2,2}, \lambda_{j,0}^{2,2}, \lambda_{j,1}^{2,2}) \to_{j \to +\infty} \left(-\frac{1}{16}, \frac{9}{16}, \frac{9}{16}, -\frac{1}{16} \right),$$

$$(\lambda_{j,2}^{1,3}, \lambda_{j,1}^{1,3}, \lambda_{j,0}^{1,3}, \lambda_{j,-1}^{1,3}) = (\lambda_{j,-3}^{3,1}, \lambda_{j,-2}^{3,1}, \lambda_{j,-1}^{3,1}, \lambda_{j,0}^{3,1}) \to_{j \to +\infty} \left(\frac{1}{16}, -\frac{5}{16}, \frac{15}{16}, \frac{5}{16} \right),$$

$$(\lambda_{j,3}^{0,4}, \lambda_{j,2}^{0,4}, \lambda_{j,1}^{0,4}, \lambda_{j,0}^{0,4}) = (\lambda_{j,-4}^{4,0}, \lambda_{j,-3}^{4,0}, \lambda_{j,-2}^{4,0}, \lambda_{j,-1}^{4,0}) \to_{j \to +\infty} \left(-\frac{5}{16}, \frac{21}{16}, -\frac{35}{16}, \frac{35}{16} \right).$$

Proof. The proof is the same as in the exponential case taking into account that $\gamma(h) = K(ah)^2 - ((ah)^4/2) + O(h^6)$. Note that we consider here the Taylor series up to degree 4, otherwise the matrix involved in the first order kriging system is not invertible. □

From the previous proposition, the asymptotical kriging weights correspond to the coefficients of the mask of degree 3 Lagrange interpolating subdivision scheme [4] with the same translation-invariant and position-dependent strategies. This scheme has been proved to uniformly converge in [4]. As previously, this is enough to ensure the uniform convergence for our scheme.

Convergence result for exponential and Gaussian-type subdivision schemes of parameter $(3, 2, 2)$ can be generalized. In a forthcoming paper [5], we show that the convergence is still ensured in the case of a scheme of parameter (D, r, r) for any $(D, r) \in \mathbb{N}^2$ with $r \leq D$.
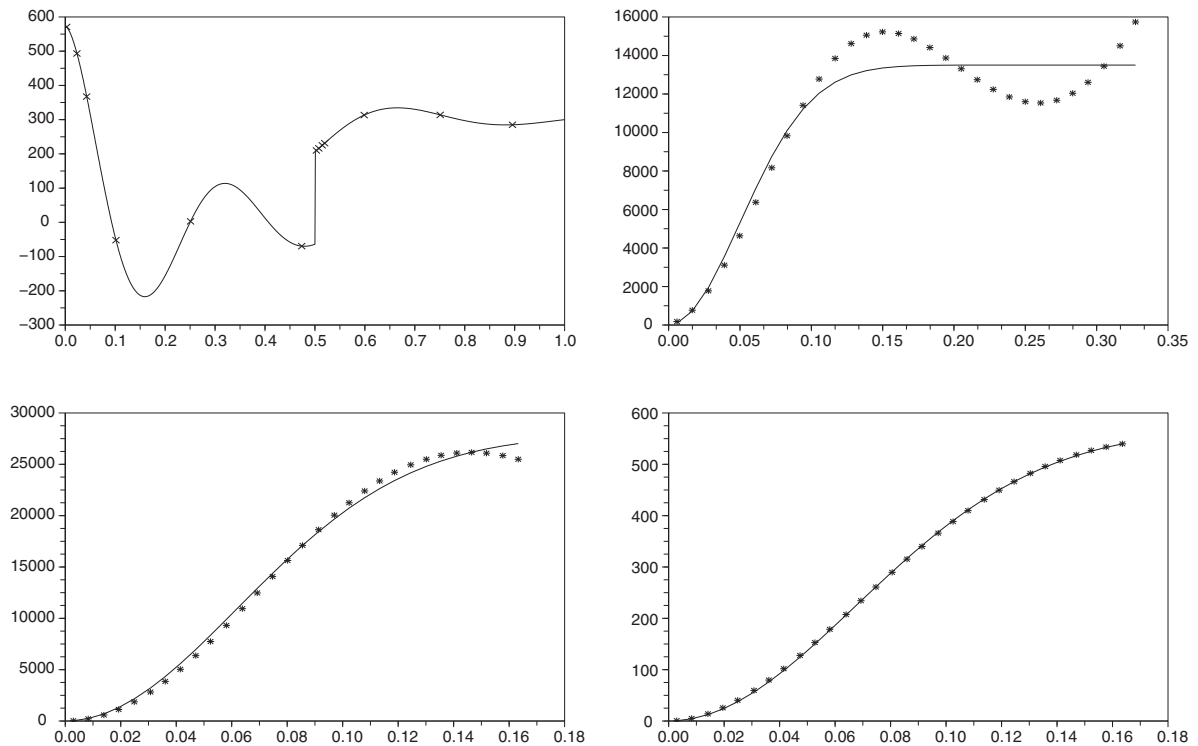
Fig. 2. Synthetic example. Top, left, synthetic data with missing information (cross signs). From top, right to bottom right, experimental (star) and theoretical (continuous line) semi-variograms for the whole data, $\gamma(h) = 2.7(1 - e^{-(1/0.7^2)h^2})$, for Zone 1, $\gamma(h) = 5.58(1 - e^{-(1/0.08^2)h^2})$ and for Zone 2, $\gamma(h) = 0.1(1 - e^{-(1/0.09^2)h^2})$.

4. Numerical tests

This section is devoted to three numerical tests. Here, the question of the accuracy of the semi-variogram identification, that refers to cross-validation techniques [7], is not addressed even though it remains a crucial point for data representation. We start by illustrating the capability of position-dependent kriging-based subdivision schemes on a synthetic example. Then, we show applications to real cases.

4.1. Synthetic example

Fig. 2, top, left, displays a synthetic set of data coming from a regular sampling ($\Delta x = 2^{-10}$) of the test function:

$$\begin{cases} 15{,}000 \dfrac{\sin(-5 + 20x)}{(5 + 20x)^2}, & \text{if } x \in \text{Zone 1} = [0; 0.5] \\ 2500 \dfrac{sin(1.5(-5 + 10(x - 1/2)))}{(5 + 20(x - 1/2))^2} + 300, & \text{if } x \in \text{Zone 2} = [0.5; 1] \end{cases}$$

Assuming that some data (cross signs) are missing, our goal is to evaluate the capabilities of our models to accurately predict this missing information.

We provide a comparison of the results obtained with the translation invariant and the position-dependent kriging-based subdivision schemes with parameters $D = 3$, $l = 2$, $r = 2$ and $y_0 = 0.5$.

The experimental and theoretical semi-variograms for each zone (position-dependent strategy) and for the whole data are plotted in Fig. 2. They have been obtained using the statistical software SUNSET developed at IRSN [6]. Note that in each case the semi-variogram exhibits a Gaussian-type structure but with different parameters.
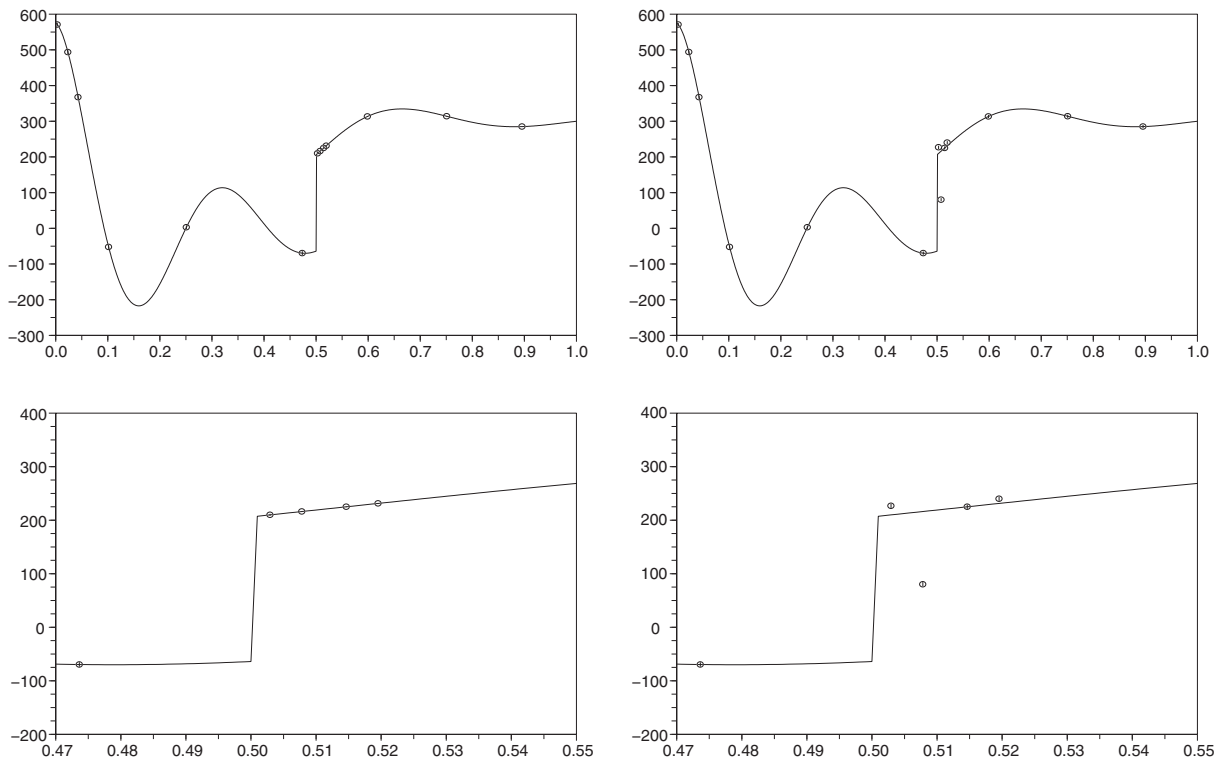
Fig. 3. Predicted data. Top, predicted data (circle) and exact measurements (continuous line) with a position-dependent (left) and translation-invariant (right) strategy. Bottom: zoom around the segmentation point.

Fig. 3 shows the predicted data while Table 1 exhibits the l^2-error and the average estimation variances.

These results point out two main advantages of position-dependent kriging-based approaches:

- The position-dependent scheme outperforms the translation-invariant one in terms of prediction. According to Fig. 3, it allows to remove oscillations (or Gibbs phenomenon) around segmentation point.
- As it can be seen in Table 1, the zone-dependent strategy drastically affects the computation of the average estimation variance. Keeping in mind that the estimation variance is related to an a priori prediction error, a refined estimation of this quantity is a real improvement of the method.

4.2. Applications to environmental data

4.2.1. Rainfall measurements

Fig. 4, top, left, displays the yearly rainfall measurements of the Sahelian zone in Gouré, Niger, Africa between 1935 and 1999 (digitalized from [12]). As in the previous example, we assume that some measurements (cross signs)

Table 1

l^2-Error and average estimation variance for a translation-invariant (TI) and a position-dependent (PD) one.

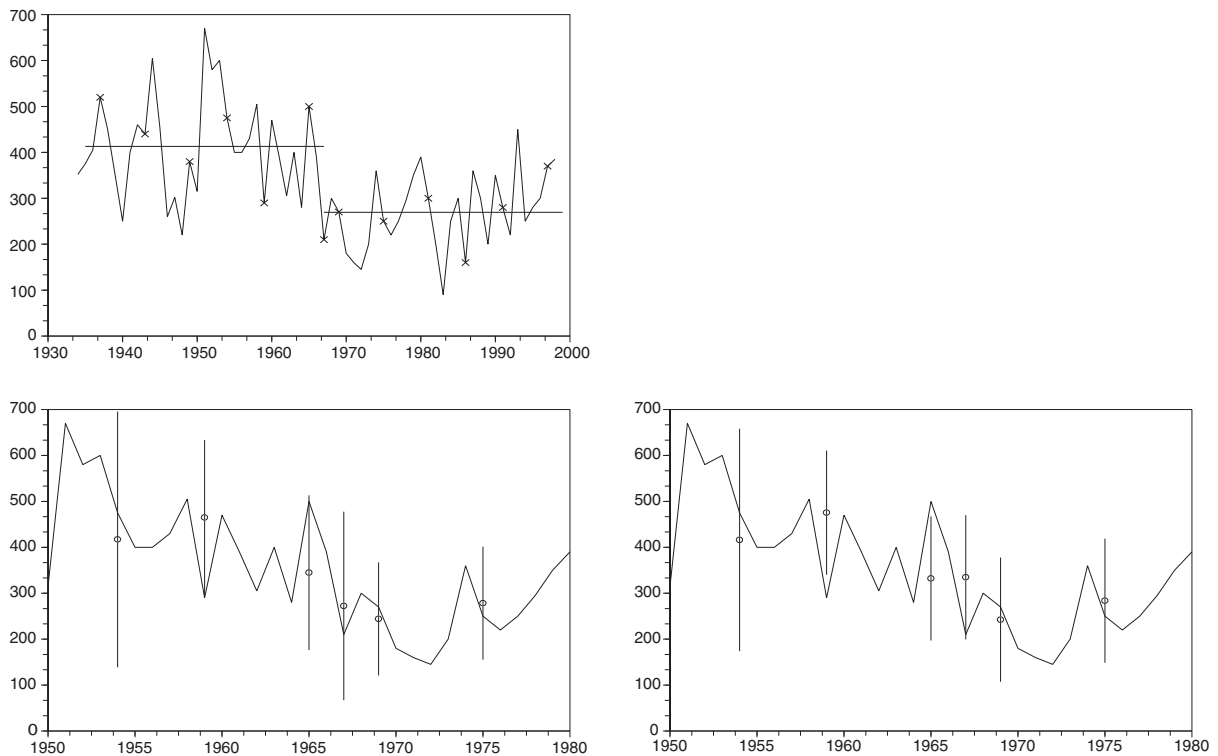| Method	l^2-Error	Average estimation variance
TI	38.1	5.1
PD	0.08	Zone 1:7, Zone 2:0.2

Fig. 4. Rainfall measurements. Top, measurements, average rainfall for each zone and missing data (cross signs). Bottom, zoom of the predicted rainfall measurements. Predicted data (circle) and exact measurements (continuous line) with prediction error (vertical line): left, position-dependent strategy, right, translation-invariant strategy.

are missing. The data of Fig. 4 exhibit two main behaviors which are confirmed by analysts: a wet period before 1967 (Zone 1) and a dry period after (Zone 2).

Following the previous approach, we compare a global kriging prediction to a two zone position-dependent one. Fig. 4 displays a zoom of the predicted data with the corresponding a priori prediction error (computed for each predicted point $f_k^{'j}$ as $I = [f_k^{'j} - 2\sigma_k^{'j}; f_k^{'j} + 2\sigma_k^{'j}]$ with $\sigma_k^{'j}$ the square root of the estimation variance).

It appears that the position-dependent approach always leads to confidence intervals encompassing the true value of the measurement, in opposition to what happens with the translation-invariant strategy.

4.2.2. Simplified example of radioactive contamination mapping

We consider here a simplified example of a radio-nuclide concentration map in a nuclear test area. The available data are given on a fixed dyadic grid of grid step 2^{-4}.

According to the measurements (Fig. 5, top, left), high concentrations of radio-nuclide are localized around ground zero area (i.e. where tests have been conducted, Zone 1) whereas there is a drastic decrease in the concentration for further measurement points (Zone 2).

Using an alternate direction strategy, a bivariate position dependent kriging based prediction has been defined and used. After identifying two semi-variograms, we provide on Fig. 5 the concentration map provided by our prediction scheme up to scale $J = 6$. In order to compare with translation-invariant strategy and since using a unique semi-variogram is not satisfactory due to strong non-regularity, we compare our scheme to the translation-invariant Lagrange interpolating scheme classically used in subdivision process [8,3].
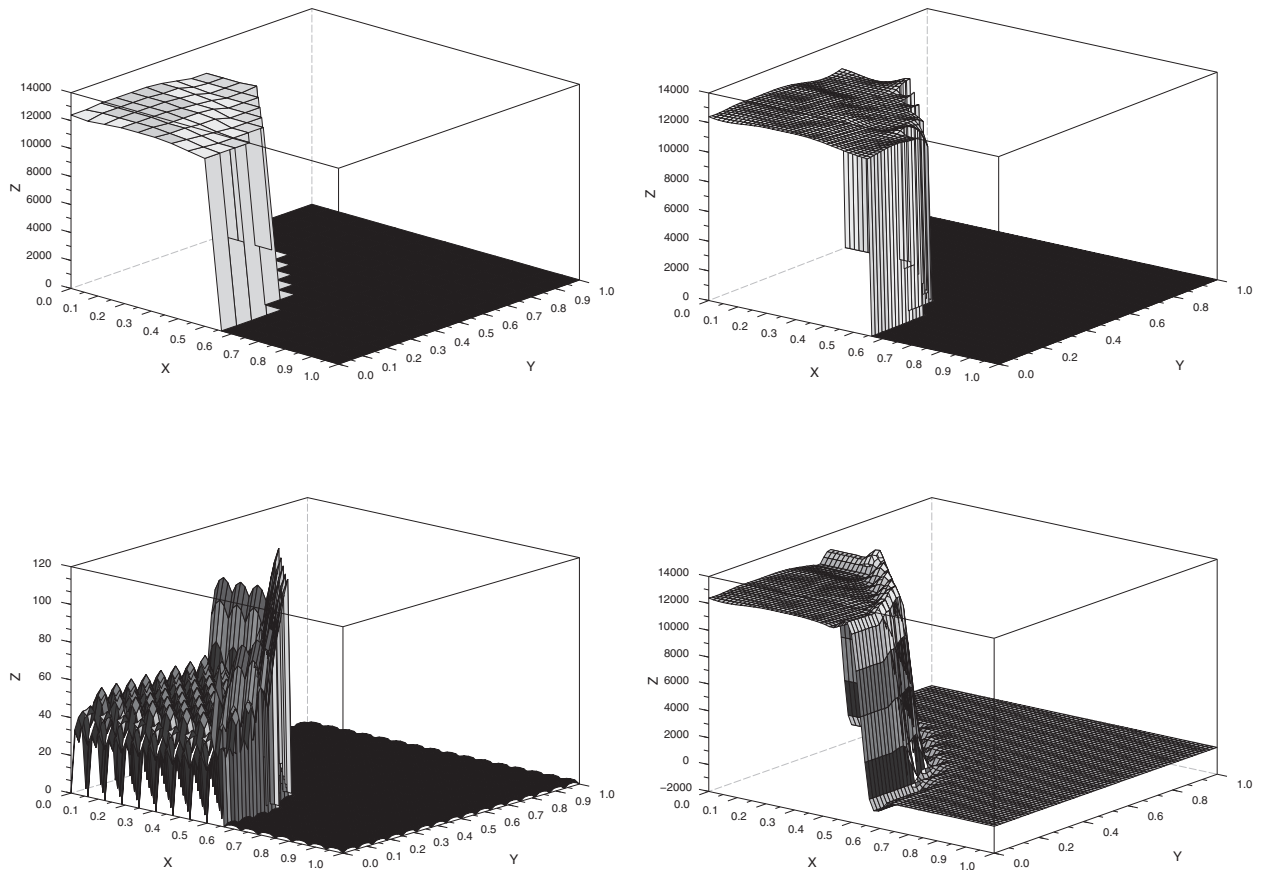
Fig. 5. Mapping of radio-nuclide concentration. Top left, initial mapping (available data) and (top right) predicted concentration map by position-dependent strategy. Bottom left, estimation standard deviation associated to the position-dependent prediction and (bottom right) concentration map provided by the classical interpolating Lagrange-based prediction.

It comes out that the removal of the Gibbs phenomenon, when performing a position-dependent strategy avoids the unrealistic negative concentrations obtained when following a translation-invariant strategy. One notes however that the model provides a bigger standard deviation along the segmentation curve, due to the extrapolation performed in the vicinity of this curve.

5. Conclusion

A new kriging-based subdivision scheme adapted to data segmentation has been introduced and fully analyzed. It is efficient for the prediction of non-regular data since it integrates a position-dependent mask taking into account the information given by the segmentation. It also provides an a priori prediction error which is relevant in risk analysis. It has been successfully applied to two environmental problems. Further developments concern the extension of this approach to non-dyadic and non-regular data grid point and its integration in a complete risk analysis study.

Appendix A.

The basic Scilab programmes to perform a 1D kriging interpolation are provided in this appendix. They concern the evaluation of the experimental semi-variogram, the identification of a theoretical one and the prediction (computation of kriging weights and estimation variance).

A.1. Estimation of the experimental semi-variogram

```
function [h_vario,vario_exp] = variogram_exp(x,z)
// Inputs: x: data location (vector)
//         z: data (vector)
// Outputs: h_vario: distance where the experimental semi-variogram
//                     is evaluated (vector)
//           vario_exp: experimental semi-variogram (vector)

//Compute the differences between observed data separated by h

n=length(x);

l=0;
for i=1:n,
      for j=i+1:n,
              l=l+1;
              difference(l)=1/2*(z(i)-z(j))*(z(i)-z(j));
              h(l)=norm(x(i)-x(j));
      end
end

//Ask for the class of distance to consider

class=input('Class boundaries for h');

//Calculate the experimental semi-variogram

N=length(class);
N_h=length(h);
M=zeros(1,N-1);
hh=zeros(1,N-1);
vario=zeros(1,N-1);

for i=1:N_h,
      for j=1:N-1,
              if h(i) >= class(j) & h(i) < class(j+1)
                     M(j)=M(j)+1;
```

```
                                            hh(j)=hh(j)+h(i);
                                            vario(j)=vario(j)+difference(i);
                                end
                        end
                end


                h_vario=[];
                vario_exp=[];

                for j=1:N-1,
                        if M(j) <> 0
                                hh(j)=hh(j)/M(j);
                                vario(j)=vario(j)/M(j);
                                h_vario=[h_vario hh(j)];
                                vario_exp=[vario_exp vario(j)];
                        end
                end

                endfunction
```

A.2. Identification of a theoretical semi-variogram

```
        // 2 valid semi-variogram models used in the applications
        // nugget effect = 0

        function [y]=expon(x,mu,C0)
        if x >0
              y=C0*(1-exp(-abs(x)/mu));
        else y =0;
        end
        endfunction

        function [y]=gauss(x,mu,C0)
        if x >0
              y=C0*(1-exp(-x/mu*x/mu));
        else y =0;
        end
        endfunction

        function [aa,err,vario_theo,name] = variogram_theo(h_vario,vario_exp,name)
        // Inputs: h_vario: distance where the experimental semi-variogram
        //                  is evaluated (vector)
        //         vario_exp: experimental semi-variogram (vector)
        //         name: semi-variogram model ('exponential' or 'gaussian')
```

```
// Outputs: aa: parameters of the identified theoretical semi-variogram
//          err: fitting error
//          vario_theo: value of the theoretical semi-variogram
//                      for h=h_vario (vector)
//          name: semi-variogram model ('exponential' or 'gaussian')


N=length(h_vario);
Z=[h_vario;vario_exp];

//Ask for the type of semi-variogram model (exponential or gaussian)

name=input('Semi-vario model?','string');

//Identification of the semi-variogram parameter

if name=='exponential'
deff('[e]=G(p,z)','e=z(2)-expon(z(1),p(1),p(2))')
[aa,err]=datafit(G,Z,[30;18000])
for i=1:N,
  vario_theo(i)=expon(h_vario(i),aa(1),aa(2));
end
end

if name=='gaussian'
deff('[e]=G(p,z)','e=z(2)-gauss(z(1),p(1),p(2))')
[aa,err]=datafit(G,Z,[50;1.0])
for i=1:N,
  vario_theo(i)=gauss(h_vario(i),aa(1),aa(2));
end
end

endfunction
```

A.3. Prediction

```
//2 valid semi-variogram models

function [y]=expon(x,mu,C0)
if x >0
     y=C0*(1-exp(-abs(x)/mu));
else y =0;
end
endfunction
```

```
function [y]=gauss(x,mu,C0)
if x >0
        y=C0*(1-exp(-x/mu*x/mu));
else y =0;
end
endfunction

function [z_new,estimation_var]=krig(x,z,x_new,name,aa)
// Inputs: x: data location (vector)
//         z: data (vector)
//         x_new: new location for interpolation
//         name: semi-variogram model ('exponential' or 'gaussian')
//         aa: parameters of the identified theoretical semi-variogram
// Outputs: z_new: interpolated data at location x_new
//          estimation_var: estimation variance


if name=='exponential'
deff('[y]=f(x)','y=expon(x,aa(1),aa(2))')
end

if name=='gaussian'
deff('[y]=f(x)','y=gauss(x,aa(1),aa(2))')
end

//Left hand side matrix of the kriging system

A=[];
n=length(X);

for i=1:n
        for j=1:n
                A(i,j)=f(abs(x(i)-x(j)));
        end
end

A(n+1,1:n+1)= (ones(n+1))';
A(1:n+1,n+1)= ones(n+1);
A(n+1,n+1)=0;

z_new=[];
estimation_var=[];

for i=1:length(x_new),

        x0=x_new(i);
```

```
//Right hand side vector of the kriging system

        for i=1:n
                F(i)=f(abs(x(i)-x0));
        end

        F(n+1)=1;

//Compute the kriging weights

        W=A^(-1)*F;
        mu=W(n+1);

//Compute the interpolated value

        z0=W(1:n)'*z;

//Compute the estimation variance

        var=mu-f(0)+W(1:n)'*F(1:n);

        z_new=[z_new;z0];
        estimation_var=[estimation_var var];

    end

    endfunction
```

References

[1] S. Amat, F. Arandiga, A. Cohen, R. Donat, G. Garcia, M. von Oehsen, Data compression with ENO schemes: a case study, Journal of Applied and Computational Harmonic Analysis 11 (2001) 273–288.
[2] S. Amat, J. Liandrat, On the stability of the pph nonlinear multiresolution, Journal of Applied and Computational Harmonic Analysis 18 (2) (2005) 198–206.
[3] F. Arandiga, R. Donat, A. Harten, Multiresolution based on weighted averages of the hat function I: linear reconstruction techniques, SIAM Journal of Scientific Computer 36 (1) (1999) 160–203.
[4] J. Baccou, J. Liandrat, Position-dependent lagrange interpolating multiresolutions, International Journal of Wavelets, Multiresolution and Information 5 (4) (2005) 513–539.
[5] J. Baccou, J. Liandrat, Kriging-based subdivision schemes, SIAM MMS, submitted for publication.
[6] E. Chojnacki, A. Ounsy, Description of the ipsn method for the uncertainty and sensitivity analysis and the associated software: Sunset, Proceedings of ASME/JSME ICONE, Louisiana 3 (1996) 545–550.
[7] N.A. Cressie, Statistics for Spatial Data. Wiley Series in Probability and Mathematical Statistics, 1993.
[8] N. Dyn, Subdivision schemes in computer-aided geometric design, in: W.A. Light (Ed.), Advances in Numerical Analysis II, Wavelets, Subdivision Algorithms and Radial Basis Functions, Clarendon Press, Oxford, 1992.
[9] P. Goovaerts, Geostatistics for Natural Resources Evaluation, Oxford University Press, 1997.
[10] A. Harten, Multiresolution representation of data: a general framework, SIAM Journal of Numerical Analysis 33 (3) (1996) 1205–1256.
[11] C.A. Miccheli, H. Prautzsch, Uniform refinement of curves, Linear Algebra and Applications 114/115 (1989) 841–870.
[12] P. Ozer, C. Bodart, B. Tychon, Climatic analysis of the gouré area, eastern niger: recent changes and environmental impacts, Cybergeo, Environment, Nature, Paysage 308 (2007).
[13] H. Wackernagel, Multivariate Geostatistics, Springer, 1998.